

Review

Polyaniline–Titanium Dioxide Heterostructures as Efficient Photocatalysts: A Review

Yongqiang Fu and Marcin Janczarek *

Institute of Chemical Technology and Engineering, Faculty of Chemical Technology, Poznan University of Technology, Berdychowo 4, 60-965 Poznan, Poland; yongqiang.fu@doctorate.put.poznan.pl

* Correspondence: marcin.janczarek@put.poznan.pl

Abstract: This review paper focuses on present issues concerning the use of polyaniline–TiO₂ heterostructures as potentially efficient photocatalysts. Conducting polymers such as polyaniline (PANI) are used in the preparation of heterojunction systems with metal oxides like titania to overcome their inherent limitations, e.g., their sole absorption of UV light and overly fast recombination of charge carriers. This review discusses preparation methods, the properties of resultant products and mechanistic aspects. An important part of this paper is its presentation of the major challenges and future perspectives of such photocatalytic materials.

Keywords: photocatalysis; titanium dioxide; polyaniline

1. Introduction

Titanium dioxide (TiO₂; titania) has been recognized as the most promising photocatalytic material, with high application potential in the fields of water or air treatment (mainly in the photooxidation of organic compounds) and in solar energy's conversion into chemical energy in the obtention of valuable products such as hydrogen and hydrocarbons [1–5]. Its main strengths include the optimal positions of conduction (CB) and valence bands (VB) in a semiconductor band structure, corresponding to the redox potentials of various important chemical transformations; its low cost and perfect stability toward photocorrosion and relative nontoxicity are the reasons for researchers' widespread interest.

However, to better utilize light (solar or artificial cheap sources, e.g., light-emitting diodes (LEDs)) and thus increase photocatalytic efficiency, it is necessary to overcome the weak points of titania. The first is the relatively wide band gap of TiO₂ (3.0–3.2 eV), which only corresponds to the photoabsorption of UV light. As this has been calculated in Abe's review, if all UV light (in solar spectrum) up to 400 nm were utilized, the solar light conversion efficiency for photocatalytic water splitting would only be 2% [4]. The possibility of utilizing visible light up to 600 nm or 800 nm will lead to efficiencies of 16% and 32%, respectively (Figure 1). The second limitation is the recombination of photogenerated charge carriers (electrons and holes), which reduces overall quantum efficiency [6]. During the recombination process, the excited electron reverts to the valence band without reacting to adsorbed species.

Many strategies have been designed to improve the photocatalytic performance of titania and overcome the above-mentioned problems. These range from intrinsic modifications of TiO₂ in fields such as particle morphology, particle size, specific surface area, porosity and density of surface or bulk defects [3,7–11] to chemical modifications. Therefore, the introduction of visible light activity into titania chemical modifications is required, although the preparation of defective titanium dioxide could also be a promising direction [3]. Most of these chemical modifications concern the metal and non-metal modification/doping of TiO₂, dye-sensitization and the design of titania–other semiconductor heterojunction systems [1,3,12–26]. In comparison to other modification strategies, the usage of non-metal components is still very promising. The use of noble metals or metal complexes could be



Citation: Fu, Y.; Janczarek, M. Polyaniline–Titanium Dioxide Heterostructures as Efficient Photocatalysts: A Review. *Crystals* **2023**, *13*, 1637. <https://doi.org/10.3390/cryst13121637>

Academic Editor: Maria Milanova

Received: 22 October 2023

Revised: 9 November 2023

Accepted: 13 November 2023

Published: 26 November 2023



Copyright: © 2023 by the authors. Licensee MDPI, Basel, Switzerland. This article is an open access article distributed under the terms and conditions of the Creative Commons Attribution (CC BY) license (<https://creativecommons.org/licenses/by/4.0/>).

an unreasonable solution because of the cost of these components, which can limit their practical applications. The use of carbon-, nitrogen-, boron- or sulfur- doping/modification is much cheaper than the metals enumerated above. It is necessary to mention that a consequence of the application of some carbon (e.g., pentaerythritol) or nitrogen (e.g., urea) precursors in the modification process of TiO₂ can be the formation of specific organic sensitizers on the titania surface, which is responsible for visible-light-induced photocatalytic activity [14,16]. Another possibility regarding the use of an organic sensitizer for titania is the application of conducting polymers such as polyaniline. The conductivity of polyaniline changes upon its addition to TiO₂; therefore, perspectives regarding the application of such materials not only focus on photocatalysis but also on other fields, e.g., metal oxide semiconductor devices and microactuators [27]. In this review, a brief overview of titania–polyaniline systems as photocatalysts is presented in relation to current knowledge and perspectives of application. This review also indicates the main problems in interpreting the research (including mechanistic aspects) and the reproducibility of the results.

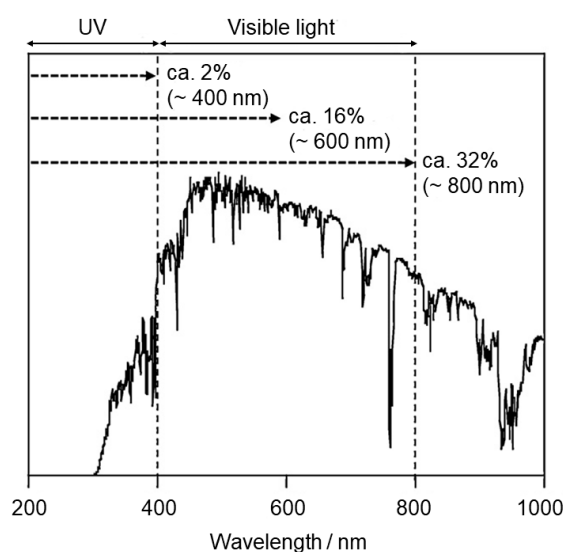


Figure 1. Solar spectrum and maximum solar light conversion efficiencies for a photocatalytic water-splitting reaction. Reprinted with permission from [4]. Copyright 2011, Elsevier.

2. Electronic and Optical Properties of Polyaniline

Polyaniline (PANI) is an example of a polymer belonging to the conducting polymer (CP) group. One can classify this group as containing electrically conducting organic polymeric compounds. Other examples of CPs are polypyrrole (PPy), polythiophene (PTh), poly(3,4-ethylenedioxythiophene) (PEDOT) and polyacetylene (PAC). CPs can act as a semiconductor or a conductor. These compounds are conjugated and show π electron delocalization along their polymer backbone. This main property determines their unique electrical and optical properties [26,28–31]. The conjugated structure of CPs is a necessary condition for the formation of delocalized electronic states. The degree of delocalization influences the value of band gap energy, which determines the conductivity of CPs. Single and double bonds contain a localized σ -bond (chemically strong). In the case of double bonds, it is also possible to distinguish a localized π -bond (less strong than the σ -bond). Therefore, π -bonds are responsible for an easier delocalization of electrons (Figure 2) [29,32].

PANI has many advantages, such as its low cost, its high environmental stability and its ability to enact electric switching between its conductive and resistive states via doping processes; it is important to emphasize that PANI is characterized by its diversity of structural forms [33]. Polyaniline is a mixed oxidation state-conducting polymer, which consists of reduced benzenoid amine units ($-\text{NH}-$) and oxidized quinoid imine units ($=\text{N}-$) (Figure 3). PANI's average oxidation state is denoted as $1 - x$. When $1 - x = 0$ PANI exists as fully reduced leucoemeraldine (LE). If the value $1 - x$ is equal to 0.5, the half-oxidized

emeraldine base (EB) is present. The fully oxidized form of PANI is pernigraniline (PE) when $1 - x = 1$ [28,34].

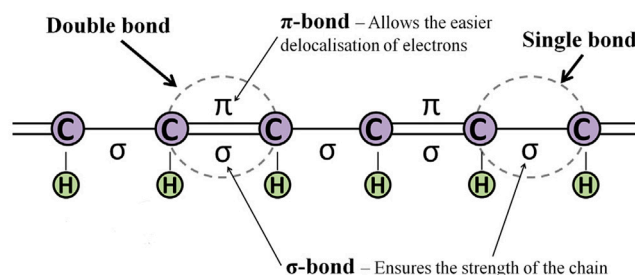


Figure 2. A representation of a conjugated backbone [32].

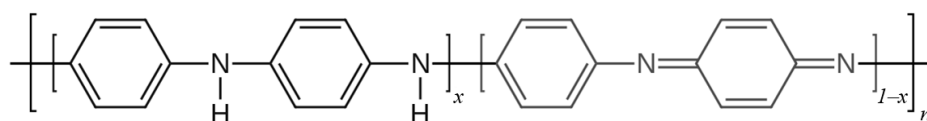


Figure 3. General structure of polyaniline.

If the EB form of PANI is doped with inorganic acids and organic acids such as phosphoric acid, hydrochloric acid, sulfosalicylic acid and sulfuric acid, emeraldine salt (ES) is then formed. In this process, imine nitrogen is protonated by acid, and the conductivity of ES significantly increases in comparison to other forms of PANI (Table 1) [35]. Furthermore, as has been presented in Table 1, enumerated forms of PANI are characterized by different values of band gap energy. The colors of these materials are white, blue/violet, blue and green for LE, PE, EB and ES, respectively [34,35].

Table 1. The main properties of different forms of PANI [34–38].

PANI Form	Conductivity/S cm ⁻¹	Band Gap Energy/eV
Leucoemeraldine	10^{-5} – 10^{-10}	3–4
Pernigraniline	10^{-5} – 10^{-10}	1.4–2.2
Emeraldine base	1–5	3–4
Emeraldine salt	30–200	2.7

The ES form of PANI is the main candidate for a good photocatalytic material, owing to its high electron transfer properties in conjunction with its low band gap energy. The reason for this can be the polaron band formation that occurs. Furthermore, the result of partial oxidation is the occurrence of crystal lattice distortion, which can be responsible for the formation of polaron and bipolaron bands. Polaron formation is due to an upward shift in the highest occupied molecular orbital (HOMO) and a downward shift in the lowest unoccupied molecular orbital (LUMO), which results in a reduction in band gap energy. In general, the π – π^* conjugate electron and polaron band transition system improves electron mobility, positively influencing photocatalytic properties through a reduction in the charge carrier recombination effect [35,39]. The low band gap is mainly due to the charge transfer exciton, such as the transition of the benzenoid rings from the HOMO (π_b) to the LUMO (π_q). Another transition, referred to as the UV region, is assigned to the $\pi_b \rightarrow \pi^*$ transition. Furthermore, ES-PANI behaves as a p-type semiconductor [37].

The optical properties of PANI are closely related to the form of PANI and preparation/modification conditions. For example, Figure 4 shows changes in the absorption spectrum of EB under different conditions of its protonation [34]. EB has an absorption peak at 2.1 eV due to electronic excitation from the benzenoid (π_b) to the quinoid rings (π_q). When pH changes to 3, absorption at 2.1 eV shifts to 1.5 eV. The reason for this is the lattice distortion of polyaniline into a polaronic structure as a result of the protonation of imine nitrogen atoms. Its peak at 3.9 eV can be attributed to the following transitions: (1) π – π^*

transition, which is similar to that of LE; (2) the transition from low-lying orbitals to the π_q orbital. However, an absorption study on the different concentrations of ES in 80% acetic acid did not show any interchain interactions [34]. Generally, regardless of the form, PANI has a high absorbance coefficient over a wide spectral range, from the Vis to IR region [35].

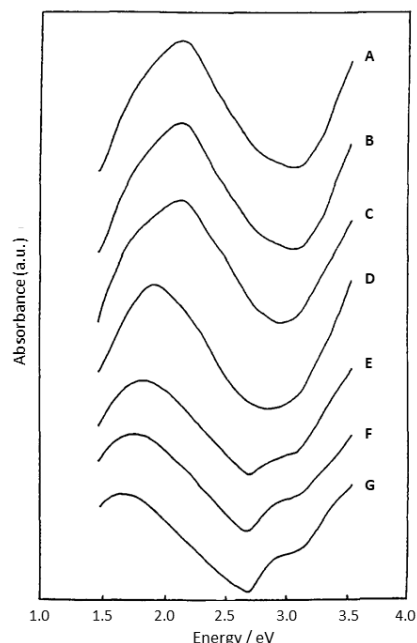


Figure 4. Changes in the photoabsorption properties of PANI (emeraldine base) during its protonation: (A) pH 6, 16 h; (B) 10^{-4} M HCl, 24 h; (C) 2×10^{-4} M HCl, 3 h; (D) 4×10^{-4} M HCl, 4.5 h; (E) 6×10^{-4} M HCl, 2 h; (F) 8×10^{-4} M HCl, 16 h; (G) 10^{-3} M HCl, 2 h. Reprinted with permission from [34]. Copyright 1993, Elsevier.

3. The Concept of Improving Photocatalytic Activity via Binary System: Metal Oxide—Polyaniline Heterostructure Nanocomposites

Referring to the previous chapter, the chemical structure and form of PANI determine its electronic and optical properties. It is known that PANI usually behaves as a p-type semiconductor. This means that PANI has an E_f (Fermi level) close to the HOMO—it can receive electrons and demonstrate downward band bending [38]. PANI has the LUMO level in the range of -1 to -2 V vs. NHE and has the HOMO level in the range of 0.4 – 0.6 V [35,37,40]. Therefore, the formation of heterojunctions between PANI and metal oxides such as TiO_2 is possible.

First, if two semiconductors with different redox energy levels are coupled, it can lead to an increase in photocatalytic performance by improving charge carrier separation. Second, it is important that the conditions for an efficient interparticle transfer between the semiconductor and TiO_2 are met; the CB of titania is more anodic than the corresponding band of the sensitizer. Then, if one only considers the visible light activation of a semiconductor–sensitizer, this component is excited, and electrons photoexcited to its CB are injected into the conduction band of the titania [22,24,41–43].

The coupling of an n-type semiconductor (e.g., TiO_2) with a p-type semiconductor (e.g., PANI) is advantageous from a photocatalytic point of view. This combination of semiconductors can ensure an efficient electron transfer between them [43]. Given the band positions of PANI and n-type semiconductors, such as metal oxides, it is possible to design a heterojunction system with a high photocatalytic performance (Figure 5, left). The band positions of PANI and TiO_2 form a type II heterojunction (staggered band pattern) (Figure 5, right). Considering the fact that PANI can be activated by visible light, the following main advantages of TiO_2 properties can be mentioned: (1) the visible light sensitization of a titania-containing system, (2) the improvement of charge carrier separation. Therefore,

a synergistic effect from these two semiconductor components can be expected. As for the PANI/TiO₂ ratio, the influence of this issue on photocatalytic activity is often studied; in most research reports, the amount of titania is higher than PANI.

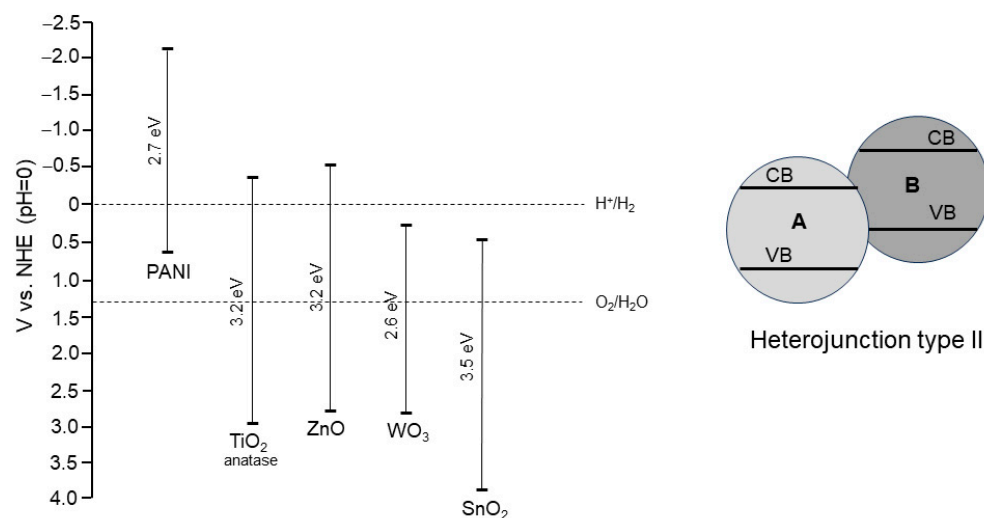


Figure 5. Band positions and band gap energies of PANI and exemplary n-type metal oxide semiconductors. Data collected from [43,44] (left). Symbolic presentation of a type II heterojunction system of coupled semiconductors; A—TiO₂, B—PANI (right).

4. PANI–TiO₂ Binary Heterojunction Systems—The State of the Art

A prospective photocatalytic material with high application potential should meet three main criteria: (1) high photocatalytic performance over a broad light spectrum in major reactions, such as the degradation of organic pollutants, hydrogen production and CO₂ reduction in high-value-added products; (2) reasonable cost for reproducible and large-scale production; (3) high stability (the retention of photocatalytic properties after many cycles). A major problem concerning these standards is that, as more components are introduced into the structure of the resultant material, its stability tends to decrease. Therefore, this review focuses on binary PANI and TiO₂ heterojunctions to better understand the great potential of this type of material. However, many examples of ternary or multicomponent composites containing both PANI and TiO₂ can be found in the literature [45–56]. Table 2 summarizes the binary PANI–TiO₂ heterostructures acting as photocatalysts. Three main areas were considered: preparation conditions, photocatalytic efficiency and aspects of the photocatalytic mechanism.

4.1. Preparation Conditions

The main method for the preparation of PANI–TiO₂ composites is the in situ chemical oxidative polymerization of aniline, using ammonium persulfate (APS) as an oxidant. This process occurs in the presence of TiO₂ or a titania precursor. Key reaction parameters, such as the molar ratio of aniline/APS and aniline/TiO₂, are different. Furthermore, polymerization conditions vary as well: polymerization time ranges from 1 h to 20 days, and process temperature ranges from ice bath conditions to room temperature. It is therefore difficult to find the optimal variant for this method. However, there are several reports that take into account the dominant amount of PANI. It is usually possible to find the best PANI/TiO₂ ratio for photocatalytic performance. Figure 6 shows this type of study with 2% PANI content as the best amount for photocatalytic activity [57]. In general, these values vary in other reports according to experimental conditions.

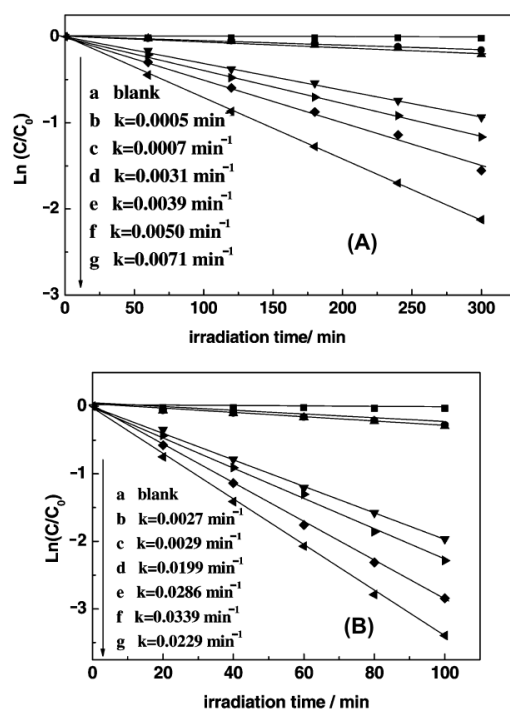


Figure 6. Plots of the photodegradation of (A) methylene blue and (B) Rhodamine B over PANI/TiO₂ photocatalysts under visible light irradiation with $\lambda > 450$ nm: (a) blank, (b) TiO₂, (c) mechanical mixture of PANI and TiO₂ (3:100), (d) PANI (1.0%)/TiO₂, (e) PANI (5.0%)/TiO₂, (f) PANI (2.0%)/TiO₂, (g) PANI (3.0%)/TiO₂. Reprinted with permission from [57]. Copyright 2008, American Chemical Society.

A much smaller number of papers consider other preparation methods. Some reports include PANI and TiO₂ impregnation procedures [58–61]. A novel, green and promising procedure for the preparation of PANI/TiO₂ was proposed by Cionti et al. [62]. Figure 7 shows the main steps of this procedure: (1) UV light-mediated growth of PANI oligomers on a TiO₂ surface, (2) polymerization of the oligomers with H₂O₂.

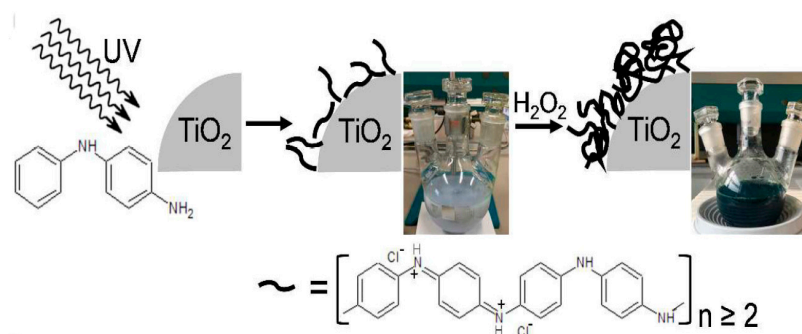


Figure 7. UV light-mediated PANI/TiO₂ preparation method. Reprinted with permission from [62]. Copyright 2018, Royal Chemical Society.

As for the form of TiO₂ that forms a part of the composites discussed, it is a commercial material in many cases, such as P25, which contains a mixture of anatase (85%) and rutile (15%). Some authors directly used a titania precursor in a polymerization procedure. Attempts have also been made to obtain special morphological forms of TiO₂, such as a self-assembled monolayer [63], mesoporous material [64–66], flowerlike NPs [67], nanotubes [68,69], nanosheets [60], nanofiber membranes [70], fiber films [59] and nanorods [71]. Some works have described the possibility of using defective forms of titania, e.g., grey or black titania [72,73]. There are also reports of modified forms of TiO₂

with noble metals such as Au, Pt and Ag [58,74–76], core–shell structures with SiO₂ [77] and combinations with reduced graphene oxide [78]. Furthermore, several applicable forms of PANI/TiO₂ have been considered, such as gypsum plasters [79], acrylic pseudo-paints [80], cotton fabric [81] and polyurethane foam [82].

The identification of the PANI form (oxidation state) present in a resultant product is not a common procedure. Only some authors include information about the PANI form. As explained earlier, the form of PANI directly affects its photocatalytic properties. Therefore, it is difficult to discuss the mechanism of photocatalytic action without this knowledge. There are also a very limited number of approaches for obtaining PANI with different morphological forms [83].

4.2. Photocatalytic Efficiency

Testing the photocatalytic efficiencies of PANI/TiO₂ is another crucial issue. As many as 65% of reports concern the use of organic dyes as model compounds, such as methylene blue, rhodamine B or methyl orange. This approach is highly controversial, especially for testing under visible light conditions [84]. The photosensitizing effect of the dye itself, induced by visible light, can cause the misconception that a given photocatalyst enacts real activity under visible light. Fortunately, authors included colorless organic compounds, such as phenol or 4-chlorophenol, in some of their reports. Another issue is the need to study the effect of dye adsorption and include this information in the graphs. Therefore, the selection of dyes as model compounds for photocatalytic experiments requires careful planning.

When the types of photocatalytic reactions are considered, most of the publications are concerned with the photocatalytic oxidation of organic compounds, and the photocatalytic efficiencies reported in both UV and Vis were high in this field, but the materials from some of the papers, especially when methylene blue was used under visible light conditions, should probably be retested, using other model compounds. As shown in Figure 8, more than 80% of 4-chlorophenol was degraded after 7 h, confirming the synergistic effect of PANI and TiO₂ [64]. Considering other reaction types, only 12% of the publications are concerned with testing hydrogen evolution process [72,75,76,78,85], and one report deals with photocatalytic reduction in carbon dioxide [86]. These reaction fields still require further research in order to test the suitability of these materials. It should be noted that most PANI/TiO₂ photocatalysts that are active in hydrogen evolution contain modified titania (with noble metals or with defective structure—grey titania). Moreover, the work of El-Bery et al. (Figure 9) demonstrated that the PANI/TiO₂ sample is more active in photocatalytic hydrogen evolution than PEDOT/TiO₂ and PPy/TiO₂, confirming the good prospects of PANI composites with titania compared to other conductive polymers [61].

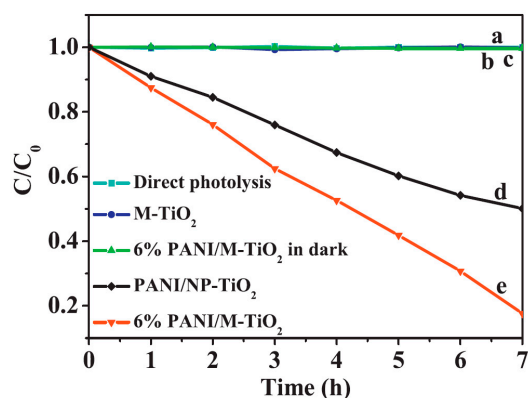


Figure 8. Photocatalytic degradation of 4-chlorophenol under visible light irradiation ($\lambda > 400$ nm); (a) direct photolysis, (b) M(mesoporous)-TiO₂, (c) 6% PANI/M-TiO₂ in the dark, (d) PANI-NP-TiO₂, (e) 6% PANI/M-TiO₂. Reprinted with permission from [64]. Copyright 2011, Elsevier.

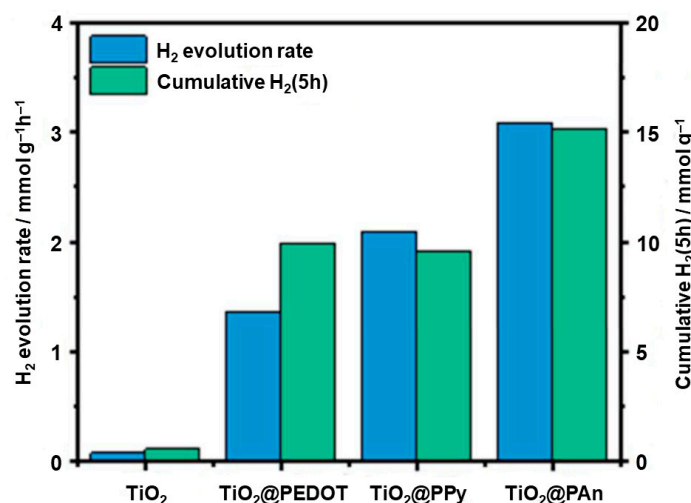


Figure 9. Comparison of TiO₂(P25), PEDOT/TiO₂, PPy/TiO₂, PANI/TiO₂ photocatalytic activities in the process of hydrogen evolution [61].

4.3. Photocatalytic Mechanism

Upon analyzing the mechanisms of photocatalytic reactions based on the PANI/TiO₂ materials presented in the publications surveyed, there is general agreement on the mechanistic routes. Figure 10 shows the mechanism of reactive oxygen species generation under UV and Vis conditions using PANI/TiO₂ photocatalysts. As shown in Figure 5, the HOMO of PANI is located between the VB and CB bands of titania, while the LUMO of PANI is located higher than the CB of TiO₂. This has been experimentally verified and reported by Hidalgo et al. [85]. Considering UV radiation (Figure 10a), both PANI and TiO₂ absorb photons. The charge is immediately transferred from the HOMO to LUMO levels in PANI. Photogenerated electrons are transferred from the LUMO of PANI to the CB of TiO₂. An electron center is formed. Charge separation is enhanced, and superoxide radicals are generated in the presence of oxygen (reduction reaction). Subsequently, these radicals react with water to form hydroxyl radicals (OH•). Simultaneously, photogenerated holes from the VB of TiO₂ migrate to the surface of the HOMO of PANI. A hole center is then formed, which is involved in the oxidation of water to OH• (oxidation reaction). The resulting reactive oxygen species (mainly hydroxyl radicals) participate in the oxidation of organic compounds. The synergistic effect of PANI and TiO₂ relates to an efficient charge carrier separation, which reduces the recombination effect and increases photocatalytic activity [87,88].

Under visible light irradiation, only the PANI component is excited (Figure 10b). The charge migrates from the HOMO to LUMO of PANI. The excited-state electrons from PANI can then be transferred from the LUMO of PANI to the CB of TiO₂. An electron center is formed. Simultaneously, the transitions $\pi \rightarrow$ polaron and polaron $\rightarrow \pi^*$ in PANI are induced. Photogenerated holes in the π orbital of PANI are transferred to the interface and react with water to form hydroxyl radicals. The synergistic effect of PANI and TiO₂ is associated not only with visible light sensitization of TiO₂ through PANI but also with improved charge separation [87,88].

There are also reports of modifications to the PANI–TiO₂ binary system. The modification of the mechanism is the result of such a concept. For example, Zhang et al. modified the PANI–TiO₂ composite with gold [58]. In this mechanism, additional hot electrons from Au NPs are injected into the CB of titania, inducing a visible-light-mediated surface plasmon resonance (LSPR) mechanism (Figure 11). The presence of Au NPs in this system enhances the charge separation and visible light sensitization effect due to the additional synergy between Au@TiO₂ and PANI–TiO₂.

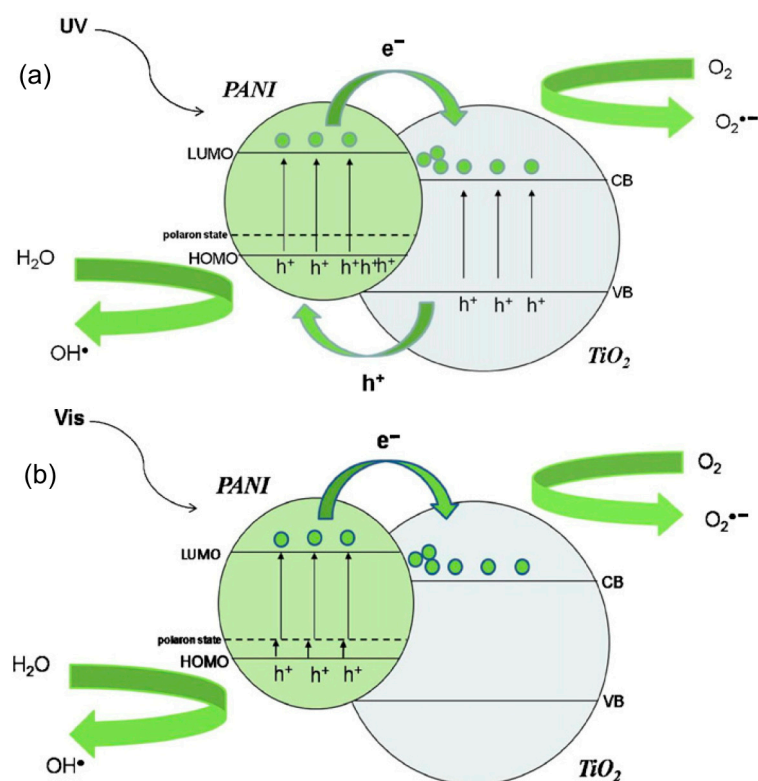


Figure 10. Mechanism of the generation of reactive oxygen species under (a) UV and (b) visible light by a PANI–TiO₂ nanocomposite photocatalyst. Reprinted with permission from [88]. Copyright 2021, Elsevier.

Table 2. Summary of binary PANI–TiO₂ heterostructures with photocatalytic properties.

PANI–TiO ₂ Material	Preparation Conditions	Photocatalytic Efficiency	Type of Photocatalytic Mechanism	Ref.
PANI/SAM-TiO ₂	A self-assembled TiO ₂ monolayer was used during aniline polymerization in the presence of HCl for 4 h; PANI was in ES form.	Photodegradation of methylene orange was performed under sunlight. Almost all the amounts of MO degraded during 150 min.	Proposed sensitization mechanism of TiO ₂ by PANI.	[63]
PANI/TiO ₂	PANI and TiO ₂ (P25) were mixed in tetrahydrofuran. An optimum synergetic effect was found for 3 wt% of PANI.	Photodegradation of methylene blue and rhodamine B was performed under UV and Vis ($\lambda > 450$ nm). The activities under Vis for the PANI/TiO ₂ (3 wt%) sample were $k = 0.0071 \text{ min}^{-1}$ (MO) and $k = 0.0229 \text{ min}^{-1}$. The activities under UV for the PANI/TiO ₂ (3 wt%) sample were $k = 0.0091 \text{ min}^{-1}$ (MO), $k = 0.099 \text{ min}^{-1}$ in comparison to pure TiO ₂ ; $k = 0.046 \text{ min}^{-1}$ (MO) and $k = 0.066 \text{ min}^{-1}$.	Proposed heterojunction, providing enhanced charge separation (UV). Proposed sensitization mechanism of TiO ₂ by PANI (Vis).	[57]
PANI/TiO ₂	Aniline (0.058 M) was used as a precursor; 1 h polymerization occurred at 25 °C in the presence of TiO ₂ (0.5 g—the best conditions) and acid—the best efficiency for H ₂ SO ₄ ; PANI was in ES form.	Photodegradation of Allura Red (ALR) and Quinoline Yellow (QY) under UV light ($\lambda = 254$ nm). $k_{\text{ALR}} = 10.7 \times 10^{-4} \text{ s}^{-1}$; $k_{\text{QY}} = 13.02 \times 10^{-4} \text{ s}^{-1}$.	Proposed heterojunction, providing enhanced charge separation.	[89]

Table 2. Cont.

PANI–TiO ₂ Material	Preparation Conditions	Photocatalytic Efficiency	Type of Photocatalytic Mechanism	Ref.
PANI/TiO ₂	Camphorsulfonic acid-doped PANI was prepared first; aniline was used as a precursor; 24 h polymerization occurred at 0°. The best mass ratio of PANI and TiO ₂ (P25) was 1:500.	Photodegradation of methylene blue was performed under visible light ($\lambda > 400$ nm). $k = 0.01515 \text{ min}^{-1}$ in comparison to pure TiO ₂ , $k = 0.00963 \text{ min}^{-1}$.	Proposed sensitization mechanism of TiO ₂ by PANI.	[90]
PANI/TiO ₂ fiber film	Aniline (0.5 g) was used as a precursor; 29 h polymerization occurred at 0° in the presence of HCl and TiO ₂ multi-pore fiber film. Photocatalytic activity correlated to the crystal structure of titania.	Photodegradation of methylene blue was performed under sunlight. MB decolorization rate, using PANI/TiO ₂ film, was nearly similar to the pristine TiO ₂ film after 240 min irradiation.	Not studied	[59]
PANI/M-TiO ₂ (core–shell)	PANI and M-TiO ₂ (mesoporous titania) were mixed in tetrahydrofuran. The optimum synergetic effect was found at 6 wt% of PANI.	Photodegradation of rhodamine B and 4-chlorophenol under visible light ($\lambda > 400$ nm). The activities for the PANI/TiO ₂ (6 wt%) sample were 99.8% (RhB, 30 min) and 82.4% (4-CP, 7 h).	The role of the core–shell structure in visible light activity.	[64]
PANI nanofibers/TiO ₂	Aniline (0.91 mL) was used as a precursor; 24 h polymerization occurred at 0° in the presence of HCl. Finally, the product was dispersed in absolute ethanol to form the nonaqueous suspension of PANI nanofibers. The PANI/TiO ₂ mass ratio of 1/100 was optimal.	Photodegradation of methylene blue and rhodamine B was performed under UV and Vis ($\lambda > 420$ nm). UV: activity (both MB and RhB) was similar to pure TiO ₂ ; Vis: activity was 8 and 2.5 times better than pure titania for MB and RhB, respectively.	UV: proposed passivation of photocatalytic activity by PANI layer; Vis: proposed sensitization mechanism of TiO ₂ by PANI.	[83]
PANI/TiO ₂	Aniline (0.09 M) was dissolved in HCl; titania precursors were added to an aniline and APS solution; subsequent hydrothermal conditions were maintained at 100 °C for 4 h; next, thermal treatment occurred at different temperatures, 100–300 °C.	Photodegradation of methyl orange was performed under UV and Vis ($\lambda > 420$ nm). The best activity for the sample calcined at 200 °C; UV: $k = 2.484 \text{ h}^{-1}$; Vis: $k = 0.5316 \text{ h}^{-1}$.	Proposed sensitization mechanism of TiO ₂ by PANI.	[91]
PANI/colloidal TiO ₂ NPs	Aniline was used as a precursor; 20-day polymerization occurred in the presence of TiO ₂ ; TiO ₂ /ANI mole had ratios of 50 (TP-50), 100 (TP-100), 150 (TP-150). TP-50: PANI-ES; TP-100: both PANI-ES and PANI-EB.	Photodegradation of MB and RhB was performed under a solar simulator. The best activity reported for TP-50/TP-100 samples: RhB completely degraded after 6 h, while MB degraded 60%.	Proposed heterojunction (UV) and sensitization mechanism (Vis).	[88]
PANI/TiO ₂	Aniline was used as a precursor; 24 h polymerization occurred at room temperature in the presence of a peroxy–titanium complex and H ₂ SO ₄ ; optimal AN/Ti ratio of 1/1; conductivity of nanocomposite: $2.08 \times 10^{-2} \text{ s cm}^{-1}$.	Photodegradation of methylene blue was performed under UV ($\lambda = 365$ nm). Almost 17% degradation occurred during 100 min.	Not studied	[92]

Table 2. Cont.

PANI–TiO ₂ Material	Preparation Conditions	Photocatalytic Efficiency	Type of Photocatalytic Mechanism	Ref.
PANI/TiO ₂ nanotubes	Aniline (2 mmol) was used as a precursor; 24 h polymerization occurred at room temperature in the presence of TiO ₂ .	Photodegradation of methyl orange and orange II was performed under UV; the synergistic effect of both components was confirmed in comparison with single PANI nanotubes.	Proposed heterojunction, providing enhanced charge separation.	[68]
PANI/TiO ₂	Aniline was used as a precursor; 24 h polymerization occurred at 4 °C in the presence of TiO ₂ ; titania/aniline ratio of 1:1 wt%; dark green composite was formed.	Photodegradation of methylene blue was performed under visible light ($\lambda > 400$ nm). More than 80% of MB degraded during 5 h; the synergistic effect of both components was confirmed in comparison with single PANI.	Proposed sensitization mechanism of TiO ₂ by PANI.	[93]
PANI/TiO ₂	Aniline (0.4 M) solution in aqueous H ₂ SO ₄ (one sample sonicated; another one without sonication); 24 h polymerization occurred at 0 °C in the presence of TiO ₂ (0.5 g).	Photodegradation of methylene blue was performed under visible light ($\lambda > 400$ nm). Photodecomposition studies of MB with PANI, TiO ₂ , PANI–TiO ₂ –S, and PANI–TiO ₂ showed efficiencies of 58, 71, 77 and 65%, respectively.	Proposed sensitization mechanism of TiO ₂ by PANI.	[94]
PANI/TiO ₂ /SiO ₂ nanofiber membranes	Aniline polymerization occurred on the surface of TiO ₂ /SiO ₂ ; aniline was dissolved in HCl solution; different polymerization times were used; PANI-ES was obtained.	Photodegradation of methyl orange blue was performed under visible light ($\lambda > 420$ nm). The best activity for the sample: PANI loading of 2.3%; 87% of MO degradation occurred during 90 min.	Proposed sensitization mechanism of TiO ₂ by PANI.	[70]
3D flowerlike TiO ₂ /PANI	Aniline was used as a precursor; polymerization for 4 h at 0 °C occurred in the presence of colloidal TiO ₂ and HCl; different Ti/ANI molar ratios were prepared: 2:1, 1:2, 1:5; dark green powder was obtained.	Photodegradation of Congo red and methyl orange was performed under UV and solar light; optimal photocatalytic performance: Ti/ANI molar ratio of 1:1: degradation under UV: 92% (MO) and 96% (CR) for 2 h, being far better than for P25 (50%); for sunlight: $k = 0.031 \text{ h}^{-1}$ (MO); $k = 0.037 \text{ h}^{-1}$ (CR) in comparison to P25: $k = 0.011 \text{ h}^{-1}$ (MO); $k = 0.012 \text{ h}^{-1}$ (CR).	UV: proposed passivation of photocatalytic activity by PANI layer; Sunlight: proposed sensitization mechanism of TiO ₂ by PANI.	[67]
PANI/TiO ₂	Aniline was used as a precursor; polymerization for 3 h occurred at 0 °C in the presence of 2.5 g TiO ₂ and HCl; hydrothermal treatment was subsequently performed; different molar ratios of TiO ₂ and aniline were used: 4:1, 2:1 and 1:1.	Photodegradation of 4-nitrophenol was performed under visible light ($\lambda > 400$ nm); the molar ratio (TiO ₂ /aniline) 2:1 was optimal for the photocatalytic performance: 90% of degradation of 4-NP.	Not studied.	[95]

Table 2. Cont.

PANI-TiO ₂ Material	Preparation Conditions	Photocatalytic Efficiency	Type of Photocatalytic Mechanism	Ref.
PANI/TiO ₂ film	PANI was first synthesized from aniline dimer with the addition of poly (sodium 4-styrenesulfonate), which was used as an emulsifying and doping agent to stabilize a structure; next, green powder of PANI was deposited in the TiO ₂ films through a dip-coating method.	Photoelectrochemical behavior was evaluated under UV-Vis, using prepared photoanodes for the water photoelectrolysis reaction in a NaOH solution; an increase in photocatalytic activity was observed compared to unmodified titania; ES form of PANI was more active than the PE form.	Enhanced electron transfer and efficient charge separation.	[85]
PANI/TiO ₂	Aniline (2.5 mmol) was used as a precursor; polymerization occurred for 12 h in the presence of various amounts of TiO ₂ with respect to aniline: 0, 5, 10, 15 and 20 wt%; dark green powder was obtained.	Photodegradations of rhodamine B, methylene blue and phenol were performed under UV light; photocatalyst with 20 wt% of titania displayed the highest activity (>80% for RhB after 3 h of irradiation). All modified photocatalysts were more active than pristine TiO ₂ .	Not studied.	[96]
PANI/MS-TiO ₂	Aniline (2.5 mmol) was used as a precursor; polymerization occurred for 12 h in the presence of 0.5 g MS (mesoporous)-TiO ₂ with respect to aniline molar ratios: 20:1, 40:1, 60:1 and 80:1.	Photodegradations of rhodamine B and methylene blue were performed under visible light ($\lambda > 400$ nm). The photodegradation efficiencies for RhB and MB were 99% and 97%, respectively, for the sample with the molar ratio (TiO ₂ /ANI) 40:1.	Proposed sensitization mechanism of TiO ₂ by PANI.	[65]
Au-PANI/TiO ₂	Aniline was used as a precursor; polymerization occurred for 12 h in the presence of 400 mg TiO ₂ and chloroauric acid; different weight ratios of aniline to titania were considered: 1/30, 1/60, 1/80, 1/100.	Photodegradation of rhodamine B was performed under visible light ($\lambda > 420$ nm). Photocatalytic efficiencies for TiO ₂ , Au-TiO ₂ and Au-PANI/TiO ₂ (1:100) were $k = 0.00379 \text{ min}^{-1}$, $k = 0.00379 \text{ min}^{-1}$ and $k = 0.01016 \text{ min}^{-1}$.	Proposed sensitization mechanism of TiO ₂ by PANI, supported by the presence of Au NPs (surface plasmon resonance effect).	[58]
PANI/TiO ₂	Aniline was used as a precursor; polymerization occurred for 24 h at room temperature in the presence of 0.8 g TiO ₂ ; different weight ratios of PANI to titania were considered: 10/1, 15/1, 20/1, 25/1. Highest conductivity occurred in sample 20/1.	Photodegradation of Reactive Red 45 was performed under UVA and solar irradiation (solar simulator). Photocatalytic activity under UVA (TOC removal) for sample 15/1 and pristine TiO ₂ were 80% and 35%; under solar irradiation, complete degradation occurred; and 83% degradation occurred for samples 15/1 and TiO ₂ during 90 min.	Not studied.	[97]
PANI/TiO ₂	Aniline was used as a precursor; polymerization occurred for 24 h at 0 °C in the presence of TiO ₂ ; different amounts of titania were used at 10, 20, 40 wt%.	Photodegradation of RB5 was performed under visible light; the best activity for the sample with 10 wt% of titania content resulted in 96% of degradation.	Proposed sensitization mechanism of TiO ₂ by PANI.	[98]

Table 2. Cont.

PANI–TiO ₂ Material	Preparation Conditions	Photocatalytic Efficiency	Type of Photocatalytic Mechanism	Ref.
Carbonized PANI/TiO ₂	Aniline was used as a precursor; polymerization occurred for 3 days in the presence of TiO ₂ ; in the next step, carbonization in argon atmosphere was performed; different mole ratios of titania/aniline were considered: 20, 50 and 80.	Photodegradations of rhodamine B and methylene blue were performed under simulated solar irradiation; photocatalytic performance was optimum for molar ratio 80:1: almost 100% of MB degradation (60 min) and 97% of RhB degradation (90 min) occurred.	The role of the carbonization process—changes in TiO ₂ structures—for the improvement of charge separation.	[99]
PANI/TiO ₂	Aniline was used as a precursor; polymerization occurred for 24 h at room temperature in the presence of 0.512 g of TiO ₂ ; different molar ratios of aniline to titania were considered: 1/6, 1/5, $\frac{1}{4}$, $\frac{1}{2}$, 1/1, 2/1, 3/1, 4/1.	Photodegradation methylene blue was performed under UV/Vis irradiation; the optimum photocatalytic performance was for the sample with molar ratio 1/5: 60% of MB degradation occurred during 180 min, and for pristine titania, it was 30%.	Proposed sensitization mechanism of TiO ₂ by PANI.	[100]
PANI/grey-TiO ₂	Aniline was used as a precursor; polymerization occurred for 3 h at 0 °C in the presence of 2 g of grey-TiO ₂ ; different weight percentages for aniline were considered: 2.5, 5 and 12 wt%.	Photodegradations of rhodamine B and hydrogen evolution were performed under visible light ($\lambda > 420$ nm). The most active sample for aniline weight content of 5 wt%; for RhB resulted in almost 100% degradation (180 min); for H ₂ evolution: 9 mmol/g after 5 h of irradiation; activities were better than for single grey-TiO ₂ .	PANI serves as a co-catalyst in promoting separation of photoinduced charges, and photoelectrons and holes can efficiently transfer at the interface of PANI and grey-TiO ₂ .	[72]
PANI/black anatase TiO ₂ (BAT)	Aniline (0.2 M) was used as a precursor; polymerization occurred for 16 h at 0–4 °C in the presence of 0.2 g of BAT.	Photodegradation of methyl orange was performed under visible light ($\lambda > 450$ nm). Photodegradation efficiency of PANI/BAT sample was better than for single BAT or single PANI: 60% of MO after 40 min.	Not studied.	[73]
HP-PANI/TiO ₂	A novel preparation procedure of highly porous (HP) PANI/TiO ₂ : (1) UV-mediated PANI oligomer growth on the TiO ₂ surface was used; (2) oligomer polymerization was conducted with H ₂ O ₂ .	Photodegradation of methyl orange was performed under UV irradiation; high photocatalytic efficiency was present for HP-PANI/TiO ₂ : 97% of degradation during 20 min of irradiation.	Not studied.	[62]
rGH-PANI/TiO ₂	PANI was obtained as a chemical; TiO ₂ in the P25 was used; reduced graphene oxide–PANI/TiO ₂ composite (rGH-PANI/TiO ₂) with a three-dimensional (3D) network structure was synthesized by a two-step method, involving a hybridization process and a water bath approach.	The photo-electro-catalytic degradation efficiencies of rGH-PANI/TiO ₂ for the degradation of phenol, 2,4-dichlorophenol, and BPA were tested under UV ($\lambda > 320$ nm); this reached 100% degradation after 7 h, 3.5 h and 4.5 h, respectively.	Proposed heterojunction, providing enhanced charge separation.	[101]

Table 2. Cont.

PANI–TiO ₂ Material	Preparation Conditions	Photocatalytic Efficiency	Type of Photocatalytic Mechanism	Ref.
PANI/TiO ₂	Aniline (1 mL) was used as a precursor; polymerization occurred for 4 h at 0 °C in the presence of 0.1 g of TiO ₂ (P25).	Photodegradation of Reactive Blue-19 was performed under UV, visible and solar light; photocatalytic efficiency was similar for all sources of light: almost 100% degradation during 120 min.	Proposed heterojunction, providing enhanced charge separation (UV). Proposed sensitization mechanism of TiO ₂ by PANI (Vis).	[87]
PANI/colloidal TiO ₂ NPs	Aniline was used as a precursor; polymerization occurred 20 days in the presence of TiO ₂ ; TiO ₂ /ANI mole ratios of 50 (TP-50), 100 (TP-100), 150 (TP-150). TP-50: PANI-ES; TP-100: both PANI-ES and PANI-EB.	Photodegradation of biologically active compounds was carried out in a cell under UV degradation; for amitriptyline, sample TP-100—45% degradation (60 min); for sulcotrione, sample TP-150 (same as pristine TiO ₂)—97% degradation (60 min); for clomazone, sample TP-150—33% degradation (60 min).	Not studied.	[102]
PANI/TiO ₂ nanotubes	Titania nanotubes (TNT) were used as a substrate for the deposition of PANI via vacuumed rotating-bed plasma-enhanced vapor deposition; different plasma powers were used: 25, 50 and 75 W.	Photodegradation of RB5 was performed under UV and visible light; under UV conditions, photoactivities for TNT, PANI(25 W)/TNT and PANI (50 W)/TNT were similar (near 100% degradation); for Vis conditions, the highest degradation was for PANI (50 W)/TNT sample (56.4% degradation).	Not studied.	[69]
PANI/TiO ₂ (acrylic pseudo-paints)	Aniline was used as a precursor; polymerization occurred for 6 h at 5 °C in the presence of 1 g of TiO ₂ ; dark green materials were obtained; for the preparation of pseudo-paint films, the aqueous dispersion of dodecyl benzene sulfonic acid and PANI/TiO ₂ were prepared and added to the acrylic latex.	Photodegradation of benzene was performed under UV and Vis light; adding nanocomposites into the acrylic film improved the photocatalytic performance under visible light but decreased activity under UV light. The photocatalytic pseudo paints containing PANI/TiO ₂ nanocomposites degraded approximately 16% benzene under visible light, suggesting its use as a practical solution for indoor air purification.	Not studied.	[80]
PANI/TiO ₂ /cotton	Aniline (0.5 mol/L) was added into a TiO ₂ homogeneous suspension; the cotton fabrics after plasma pretreatment underwent the “dip-pad” method with the solution mentioned. Aniline-adsorbed cotton fabrics were immersed in a solution containing APS, and a polymerization process was conducted for 4 h at 0 °C.	Photodegradation of Rhodamine B was performed under simulated sunlight; PANI/TiO ₂ /cotton composite fabric had good adsorption and photocatalytic performance, and the total efficiency of adsorption and degradation for RhB was up to 87.7%.	Not studied.	[81]

Table 2. Cont.

PANI–TiO ₂ Material	Preparation Conditions	Photocatalytic Efficiency	Type of Photocatalytic Mechanism	Ref.
PANI/Ti _{0.91} O ₂	PANI NPs were introduced into the interlayer space of titanate lattice by the addition of Ti _{0.91} O ₂ colloidal suspension to the turbid PANI NPs suspension, stirring for 2 h; green products were obtained.	Photodegradation of Rhodamine B was performed under visible light ($\lambda > 420$ nm). Photocatalytic efficiency resulted in an almost complete degradation during 6 h.	Proposed sensitization mechanism of Ti _{0.91} O ₂ by PANI.	[60]
PANI/Pt-TiO ₂	Pt-loaded TiO ₂ NPs were prepared via photoreduction method; next, aniline was used as a precursor; polymerization occurred for 6 h at 0 °C in the presence of 0.5 g of Pt-TiO ₂ ; aniline/titania ratio was 4/100.	Photocatalytic hydrogen generation was performed under visible light ($\lambda > 420$ nm). The rates of hydrogen evolution ($\mu\text{mol h}^{-1} \text{g}^{-1}$) for TiO ₂ , Pt-TiO ₂ , PANI–TiO ₂ and PANI/Pt-TiO ₂ were 0, 0, 3 and 60, respectively.	Proposed sensitization mechanism of Pt-TiO ₂ by PANI.	[76]
PANI/M-TiO ₂	Aniline was used as a precursor; polymerization occurred for 12 h at 0 °C in the presence of 1.04 g of mesoporous TiO ₂ ; by varying aniline amounts, samples with different content of PANI were obtained: 1, 3, 5, 7, 10 wt%.	Photocatalytic reduction of Cr(VI) to Cr(III) was performed under UV; the maximum reaction rate was 0.62 min ^{−1} for samples containing 3 wt% of PANI.	Proposed heterojunction, providing enhanced charge separation.	[66]
PANI/TiO ₂ -rGO	Aniline (in different amounts: 0.225 mmol, 0.45 mmol, 0.9 mmol) was used as a precursor; polymerization occurred for 24 h at 5 °C in the presence of TiO ₂ -rGO (rGO-reduced graphene oxide); dark green material was obtained.	Photodegradations of Rhodamine B and hydrogen production were performed under visible light ($\lambda > 420$ nm); photodegradation efficiencies after 90 min of irradiation for TiO ₂ , TiO ₂ -rGO, PANI/TiO ₂ -rGO(0.225), PANI/TiO ₂ -rGO(0.45), PANI/TiO ₂ -rGO (0.9) were 22%, 62%, 80%, 90% and 85%, respectively; hydrogen production efficiencies for TiO ₂ , TiO ₂ -rGO, PANI/TiO ₂ -rGO(0.225), PANI/TiO ₂ -rGO(0.45), PANI/TiO ₂ -rGO (0.9) were (in mmol h ^{−1} g ^{−1}) 0.08, 0.45, 0.57, 0.8 and 0.72, respectively.	The enhanced photocatalytic performance is attributed to the rapid photoinduced charge separation and efficiently suppressed charge recombination caused by the synergy between PANI, TiO ₂ , and rGO. Moreover, the interfacial charge transfer in PANI and rGO with the p-conjugated group used for photocatalytic performance is of great significance.	[78]
PANI/TiO ₂	Aniline was used as a precursor; polymerization occurred overnight in the presence of TiO ₂ ; different contents of titania were used (0.2 M, 0.3 M, 0.4 M, 0.5 M, 0.6 M).	Photodegradation of methylene blue was performed under UV; For samples containing 0.6 M of titania, the efficiency was highest (86.35%), because large amounts of TiO ₂ in the PANI matrix can produce many reactive sites.	Proposed heterojunction, providing enhanced charge separation and visible light activity.	[103]
PANI/TiO ₂ nanorods	The first step: synthesis of titania nanorods (hydrothermal conditions); the second step: using aniline as a precursor; polymerization occurred for 12 h in the presence of TiO ₂ nanorods; green product was obtained.	Photodegradation of bisphenol A was performed under UV; photocatalytic efficiency was higher for PANI/TiO ₂ than for TiO ₂ : 79.8% and 60.7% of bisphenol A degradation after 80 min.	Proposed heterojunction, providing enhanced charge separation.	[71]

Table 2. Cont.

PANI-TiO ₂ Material	Preparation Conditions	Photocatalytic Efficiency	Type of Photocatalytic Mechanism	Ref.
PANI/TiO ₂ -gypsum plaster	Aniline was used as a precursor; polymerization occurred for 24 h at 0 °C in the presence of TiO ₂ (molar ratio of aniline to titania was 1:5); the photocatalytic gypsum plaster was prepared by blending commercial gypsum plaster and distilled water to obtain a paste form; PANI-TiO ₂ in 10 wt% to the dry mass of the plaster.	Photodegradation of phenol was performed under UV/Vis and visible light ($\lambda > 400$ nm and $\lambda > 420$ nm), using non-gypsum materials; UV/Vis—TiO ₂ : 4.63 $\mu\text{mol h}^{-1}$, PANI-TiO ₂ : 2.01 $\mu\text{mol h}^{-1}$, Vis(400)—TiO ₂ : 0.4 $\mu\text{mol h}^{-1}$, PANI-TiO ₂ : 0.07 $\mu\text{mol h}^{-1}$, Vis(420): TiO ₂ : 0.12 $\mu\text{mol h}^{-1}$, PANI-TiO ₂ : 0.26 $\mu\text{mol h}^{-1}$; photodegradation of toluene in the presence of gypsum plasters containing composites; using 460 nm LED activity of the gypsum containing PANI-TiO ₂ was higher than the one containing TiO ₂ ; this was the opposite if 380 nm LED was used.	Proposed heterojunction, providing enhanced charge separation and visible light activity.	[79]
PANI/TiO ₂	Aniline was used as a precursor; polymerization occurred for 12 h in the presence of TiO ₂ ; PANI contents were: 3%, 10%, 30%; green powder was formed; prepared composite (3 wt%) was added to polystyrene dissolved in toluene.	Polystyrene composite sheets were exposed to UV radiation ($\lambda = 253$ nm); the optimum photodegradation performance was reported for TiO ₂ -10% PANI, and it was almost two times higher than for single TiO ₂ .	Proposed heterojunction, providing enhanced charge separation.	[104]
Polyurethane-PANI/TiO ₂	Different methods of combining polyurethane foam with PANI/TiO ₂ to form floating composites were used: (1) in situ polymerization, (2) immobilization, (3) in situ UV-assisted polymerization, (4) impregnation by organic dopant-modified PANIs solutions.	Photodegradation of Rhodamine B was performed under simulated sunlight; the composite prepared by method (4) had the best activity: almost 100% of RhB degradation occurred during 30 min.	Not studied.	[82]
PANI/TiO ₂	PANI synthesis: aniline was used as a precursor; polymerization occurred for 6 h at 5 °C; next step—the impregnation of PANI and TiO ₂ , using porcelain crucible and a DMF solution.	Photocatalytic hydrogen production was performed under UV light (LED). The highest efficiency was for samples with 5 wt% content of PANI; 15 mmol g ⁻¹ of hydrogen evolved during 5 h; this result was better than for other titania composites containing different conducting polymers such as PEDOT (10 mmol g ⁻¹) and PPy (9.5 mmol g ⁻¹).	Proposed sensitization mechanism of TiO ₂ by PANI.	[61]
PANI/TiO ₂ -Ag	The first step: the preparation of Ag-TiO ₂ NPs; The second step: the use of aniline as a precursor; polymerization occurred for 4 h in ice bath conditions in the presence of Ag-TiO ₂ ; different amounts of Ag-TiO ₂ were used: 5 wt%, 9 wt%, 11 wt% and 13 wt%.	Photocatalytic disinfection activity was tested using <i>E. coli</i> under visible light; the best sample for disinfection efficiency was a composite with 13 wt% content of Ag-TiO ₂ ; photodegradation of lipopolysaccharides were performed under visible light; ca. 40% of endotoxin was degraded in 180 min.	Not studied.	[74]

Table 2. Cont.

PANI–TiO ₂ Material	Preparation Conditions	Photocatalytic Efficiency	Type of Photocatalytic Mechanism	Ref.
PANI/SiO ₂ @TiO ₂	The first step was the preparation of core–shell SiO ₂ @TiO ₂ particles; subsequently, PANI was deposited on SiO ₂ @TiO ₂ ; aniline was used as a precursor; polymerization occurred in the presence of SiO ₂ @TiO ₂ ; molar ratios between aniline and TiO ₂ were as follows: 1:80, 1:60, 1:40; mesoporous and non-porous SiO ₂ were used.	Photodegradation of phenol was tested under visible light (LED). The highest photocatalytic performance was reported in samples with 1:80 molar ratio and a mesoporous core; 35% of phenol degradation occurred during 190 min.	Not studied.	[77]
PANI/TiO ₂ -Au	Polymeric nanocomposite films were produced via layer-by-layer technique using poly(allyamine hydrochloride), poly(acrylic acid), TiO ₂ NPs, tetrachloroauric(III) acid and mercaptoethane sodium sulfonate solutions; the films were assembled on FTO glass; PANI was in the form of ES.	Photocatalytic reaction for hydrogen production was performed in a quartz reactor, using a solar simulator; hydrogen evolution rate for the best sample was 1300 $\mu\text{mol g}^{-1}$ during 180 min.	Proposed sensitization mechanism of TiO ₂ by PANI, supported by the presence of Au NPs (surface plasmon resonance effect).	[75]
PANI/TiO ₂	Aniline (1 mL) was used as a precursor; polymerization occurred for 4 h in the presence of TiO ₂ (P25); different weight contents of titania were considered: 9.4%, 12%, 18.2%, 29.1% and 35%.	Photocatalytic reduction in carbon dioxide was performed under visible light; the yield of formaldehyde and formic acid formed per gram of catalyst increased as the TiO ₂ content in the PANI–TiO ₂ nanocomposites varied from 9.4% to 18.2%; however, a further increase in TiO ₂ content to 29.1 or 35% resulted in a decrease in the yields of products (formaldehyde and formic acid).	Proposed heterojunction, providing enhanced charge separation and visible light activity.	[86]
PANI/TiO ₂ , PANI/TiO ₂ /GO	Combination of aniline, titanium isopropoxide and graphene oxide; polymerization occurred for 2 h; finally, HCl treatment was used to obtain conductive PANI.	Photodegradations of Thymol Blue and Rose Bengal dyes were performed under visible light; the photodegradation efficiencies of TiO ₂ /PANI/GO, TiO ₂ /PANI, and TiO ₂ for Thymol Blue were 96%, 87% and 21%, respectively, after irradiation for 180 min; for Rose Bengal, they were 97%, 93% and 14%, respectively.	Not studied.	[105]
PANI/TiO ₂	PANI-ES/TiO ₂ composites were synthesized via in situ chemical oxidation polymerization method.	Photodegradation of RfOM (refractory organic matter) was performed under simulated sunlight; the synergistic effect between PANI and TiO ₂ was more pronounced in lower PANI ratios, whereas higher PANI ratios reflected a retardation effect up to a specific mass ratio of polyaniline to TiO ₂ .	Not studied.	[106]

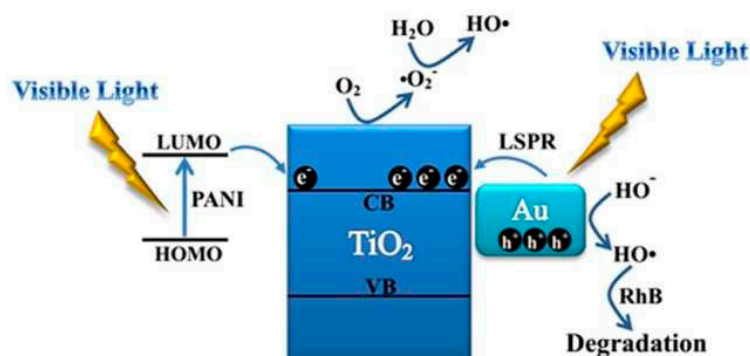


Figure 11. Mechanism of the photocatalytic degradation of RhB by the Au-PANI@TiO₂ NPs under visible light irradiation. Reprinted with permission from [58]. Copyright 2016, Royal Chemical Society.

5. Conclusions

Binary PANI–TiO₂ heterostructures are very promising photocatalytic materials. They can be used in many types of reactions, such as the photooxidation of organic compounds, photocatalytic hydrogen generation and carbon dioxide reduction. These materials can be efficient in both UV and Vis due to the synergistic effect of both components. This effect manifests itself in two aspects: (1) the presence of PANI as an effective visible light sensitizer of titania and (2) the formation of a heterojunction (type II) between PANI and TiO₂, which is a decisive factor in reducing the charge carrier recombination effect and increasing the efficiency of UV-induced reactions. Based on the literature survey, the following conclusions and remarks can be drawn: (I) there are reports on the use of different morphological forms of titania, but there are still too few reports on the influence of different forms of TiO₂ used in heterostructures with PANI on the efficiency of these binary systems; (II) there are almost no reports on the evaluation of the influence of PANI with different properties, e.g., particle size on photocatalytic activity, including the use of different preparation methods of PANI or PANI–TiO₂ heterostructures; (III) the model organic compounds in the photooxidation reactions were mainly dyes, making it advisable to use other, preferably colorless, organics, e.g., phenols, especially for visible light-induced reactions; (IV) mechanistic studies of photocatalytic reactions based on PANI–TiO₂ materials should be further investigated via experiments to confirm existing concepts or to propose other mechanism variants; (V) research into alternative, simple and low-cost preparation methods of PANI–TiO₂ structures with high application potential is highly desirable; (VI) studies on the stability of these heterostructures should be more frequently included in research reports.

Author Contributions: Y.F. and M.J. wrote the paper. All authors have read and agreed to the published version of the manuscript.

Funding: This research was supported by the Polish Ministry of Education and Science subsidy from the Poznan University of Technology.

Conflicts of Interest: The authors declare no conflict of interest.

References

- Schneider, J.; Matsuoka, M.; Takeuchi, M.; Zhang, J.; Horiuchi, Y.; Anpo, M.; Bahnemann, D.W. Understanding TiO₂ photocatalysis: Mechanisms and materials. *Chem. Rev.* **2014**, *114*, 9919–9986. [[CrossRef](#)] [[PubMed](#)]
- Nakata, K.; Fujishima, A. TiO₂ photocatalysis: Design and applications. *J. Photochem. Photobiol. C* **2012**, *13*, 169–189. [[CrossRef](#)]
- Pelaez, M.; Nolan, N.T.; Pillai, S.C.; Seery, M.K.; Falaras, P.; Kontos, A.G.; Dunlop, P.S.M.; Hamilton, J.W.J.; Byrne, J.A.; O’Shea, K.; et al. A review on the visible light active titanium dioxide photocatalysts for environmental applications. *Appl. Catal. B Environ.* **2012**, *125*, 331–349. [[CrossRef](#)]
- Abe, R. Recent progress on photocatalytic and photoelectrochemical water splitting under visible light irradiation. *J. Photochem. Photobiol. C* **2011**, *11*, 179–209. [[CrossRef](#)]
- Hossen, M.A.; Solayman, H.M.; Leong, K.H.; Sim, L.C.; Yaacof, N.; Aziz, A.A.; Wu, L.; Monir, M.U. Recent progress in TiO₂-Based photocatalysts for conversion of CO₂ to hydrocarbon fuels: A systematic review. *Results Eng.* **2022**, *16*, 100795. [[CrossRef](#)]

6. Choi, W.; Termin, A.; Hoffmann, M.R. The role of metal ion dopants in quantum-sized TiO₂: Correlation between photoreactivity and charge carrier recombination dynamics. *J. Phys. Chem.* **1994**, *98*, 13669–13679. [[CrossRef](#)]
7. Yang, H.G.; Sun, C.H.; Qiao, S.Z.; Zou, J.; Liu, G.; Smith, S.C.; Cheng, H.M.; Lu, G.Q. Anatase TiO₂ single crystals with a large percentage of reactive facets. *Nature* **2008**, *453*, 638–641. [[CrossRef](#)] [[PubMed](#)]
8. Janczarek, M.; Kowalska, E.; Ohtani, B. Decahedral-shaped anatase titania photocatalyst particles: Synthesis in a newly developed coaxial-flow gas-phase reactor. *Chem. Eng. J.* **2016**, *289*, 502–512. [[CrossRef](#)]
9. Nowotny, M.K.; Sheppard, L.R.; Bak, T.; Nowotny, J. Defect chemistry of titanium dioxide. Application of defect engineering in processing of TiO₂-based photocatalysts. *J. Phys. Chem. C* **2008**, *112*, 5275–5300. [[CrossRef](#)]
10. Bak, T.; Nowotny, J.; Sucher, N.J.; Wachsman, E. Effect of crystal imperfections on reactivity and photoreactivity of TiO₂ (rutile) with oxygen, water, and bacteria. *J. Phys. Chem. C* **2011**, *115*, 15711–15738. [[CrossRef](#)]
11. Liu, N.; Schneider, C.; Freitag, D.; Zolnhofer, E.M.; Meyer, K.; Schmuki, P. Noble-metal-free photocatalytic H₂ generation: Active and inactive ‘black’ TiO₂ nanotubes and synergistic effects. *Chem. Eur. J.* **2016**, *22*, 13810–13814. [[CrossRef](#)] [[PubMed](#)]
12. Etacheri, V.; Di Valentin, C.; Schneider, J.; Bahnemann, D.; Pillai, S.C. Visible-light activation of TiO₂ photocatalysts: Advances in theory and experiments. *J. Photochem. Photobiol. C Photochem. Rev.* **2015**, *25*, 1–29. [[CrossRef](#)]
13. Sakthivel, S.; Kisch, H. Daylight photocatalysis by carbon-modified titanium dioxide. *Angew. Chem. Int. Ed.* **2003**, *42*, 4908–4911. [[CrossRef](#)] [[PubMed](#)]
14. Zabek, P.; Eberl, J.; Kisch, H. On the origin of visible light activity in carbon-modified titania. *Photochem. Photobiol. Sci.* **2009**, *8*, 264–269. [[CrossRef](#)]
15. Kisch, H.; Sakthivel, S.; Janczarek, M.; Mitoraj, D. A low-band gap, nitrogen-modified titania visible-light photocatalyst. *J. Phys. Chem. C* **2007**, *111*, 11445–11449. [[CrossRef](#)]
16. Mitoraj, D.; Kisch, H. On the mechanism of urea-induced titania modification. *Chem. Eur. J.* **2010**, *16*, 261–269. [[CrossRef](#)]
17. Kowalska, E.; Prieto Mahaney, O.O.; Abe, R.; Ohtani, B. Visible-light-induced photocatalysis through surface plasmon excitation of gold on titania surfaces. *Phys. Chem. Chem. Phys.* **2010**, *12*, 2344–2355. [[CrossRef](#)]
18. Asahi, R.; Morikawa, T.; Irie, H.; Ohwaki, T. Nitrogen-doped titanium dioxide as visible-light-sensitive photocatalyst: Designs, developments, and prospects. *Chem. Rev.* **2014**, *114*, 9824–9852. [[CrossRef](#)]
19. Zielinska-Jurek, A.; Wysocka, I.; Janczarek, M.; Stampor, W.; Hupka, J. Preparation and characterization of Pt–N/TiO₂ photocatalysts and their efficiency in degradation of recalcitrant chemicals. *Sep. Purif. Technol.* **2015**, *156*, 369–378. [[CrossRef](#)]
20. Dozzi, M.V.; Artiglia, L.; Granozzi, G.; Ohtani, B.; Selli, E. Photocatalytic activity vs structural features of titanium dioxide materials singly doped or codoped with fluorine and boron. *J. Phys. Chem. C* **2014**, *118*, 25579–25589. [[CrossRef](#)]
21. Diaz-Angulo, J.; Gomez-Bonilla, I.; Jimenez-Tohapanta, C.; Mueses, M.; Pinzon, M.; Machuca-Martinez, F. Visible-light activation of TiO₂ by dye-sensitization for degradation of pharmaceutical compounds. *Photochem. Photobiol. Sci.* **2019**, *18*, 897–904. [[CrossRef](#)] [[PubMed](#)]
22. Bessekhoud, Y.; Robert, D.; Weber, J.-V. Photocatalytic activity of Cu₂O/TiO₂, Bi₂O₃/TiO₂ and ZnMn₂O₄/TiO₂ heterojunctions. *Catal. Today* **2005**, *101*, 315–321. [[CrossRef](#)]
23. Janczarek, M.; Endo, M.; Zhang, D.; Wang, K.; Kowalska, E. Enhanced photocatalytic and antimicrobial performance of cuprous oxide/titania: The effect of titania matrix. *Materials* **2018**, *11*, 2069. [[CrossRef](#)] [[PubMed](#)]
24. Meng, S.; Sun, W.; Zhang, S.; Zheng, X.; Fu, X.; Chen, S. Insight into the transfer mechanism of photogenerated carriers for WO₃/TiO₂ heterojunction photocatalysts: Is it the transfer of band–band or Z-scheme? Why? *J. Phys. Chem. C* **2018**, *122*, 26326–26336. [[CrossRef](#)]
25. He, F.; Zhu, B.; Cheng, B.; Yu, J.; Ho, W.; Macyk, W. 2D/2D/0D TiO₂/C₃N₄/Ti₃C₂ MXene composite S-scheme photocatalyst with enhanced CO₂ reduction activity. *Appl. Catal. B Environ.* **2020**, *272*, 119006. [[CrossRef](#)]
26. Ghosh, S.; Remita, H.; Basu, R.N. Conducting polymers nanostructures for solar-light harvesting. In *Visible Light-Active Photocatalysis: Nanostructured Catalyst Design, Mechanisms, and Applications*; Wiley: Hoboken, NJ, USA, 2018; pp. 227–252. [[CrossRef](#)]
27. Dey, A.; De, S.; De, A.; De, S.K. Characterization and dielectric properties of polyaniline–TiO₂ nanocomposites. *Nanotechnology* **2004**, *15*, 1277–1283. [[CrossRef](#)]
28. Molapo, K.M.; Ndingili, P.M.; Ajayi, R.F.; Mbambisa, G.; Mailu, S.M.; Njomo, N.; Maskini, M.; Baker, P.; Iwuoha, E.I. Electronics of conjugated polymers (I): Polyaniline. *Int. J. Electrochem. Sci.* **2012**, *7*, 11859–11875. [[CrossRef](#)]
29. Abdelhamid, M.E.; O’Mullane, A.P.; Snook, G.A. Storing energy in plastics: A review on conducting polymers & their role in electrochemical energy storage. *RSC Adv.* **2015**, *5*, 11611–11626.
30. Ghosh, S.; Kouame, N.A.; Remita, S.; Ramos, L.; Goubard, F.; Aubert, P.-H.; Dazzi, A.; Deniset-Besseau, A.; Remita, H. Visible-light active conducting polymer nanostructures with superior photocatalytic activity. *Sci. Rep.* **2015**, *5*, 18002. [[CrossRef](#)]
31. Kang, E.T.; Neoh, K.G.; Tan, K.L. Polyaniline: A polymer with many interesting intrinsic redox states. *Prog. Polym. Sci.* **1998**, *23*, 277–324. [[CrossRef](#)]
32. Balint, R.; Cassidy, N.J.; Cartmell, S.H. Conductive polymers: Towards a smart biomaterial for tissue engineering. *Acta Biomater.* **2014**, *10*, 2341–2353. [[CrossRef](#)]
33. Kaur, G.; Adhikari, R.; Cass, P.; Bown, M.; Gunatillake, P. Electrically conductive polymers and composites for biomedical applications. *RSC Adv.* **2015**, *5*, 37553–37567. [[CrossRef](#)]
34. Huang, W.S.; MacDiarmid, A.G. Optical properties of polyaniline. *Polymer* **1993**, *34*, 1833–1845. [[CrossRef](#)]

35. Ekande, O.S.; Kumar, M. Review on polyaniline as reductive photocatalyst for the construction of the visible light active heterojunction for the generation of reactive oxygen species. *J. Environ. Chem. Eng.* **2021**, *9*, 105725. [[CrossRef](#)]
36. Kwon, O.; McKee, M.L. Calculations of band gaps in polyaniline from theoretical studies of oligomers. *J. Phys. Chem. B* **2000**, *104*, 1686–1694. [[CrossRef](#)]
37. Belabed, C.; Abdi, A.; Benabdelghani, Z.; Rekhila, G.; Etxeberria, A.; Trari, M. Photoelectrochemical properties of doped polyaniline: Application to hydrogen photoproduction. *Int. J. Hydrogen Energy* **2013**, *38*, 6593–6599. [[CrossRef](#)]
38. Huang, H.G.; Zheng, Z.X.; Luo, J.; Zhang, H.P.; Wu, L.L.; Lin, Z.H. Internal photoemission in polyaniline revealed by photoelectrochemistry. *Synth. Met.* **2001**, *123*, 321–325. [[CrossRef](#)]
39. Deb, K.; Bera, A.; Saha, B. Tuning of electrical and optical properties of polyaniline incorporated functional paper for flexible circuits through oxidative chemical polymerization. *RSC Adv.* **2016**, *6*, 94795–94802. [[CrossRef](#)]
40. Chen, S.; Huang, D.; Zeng, G.; Gong, X.; Xue, W.; Li, J.; Li, T. Modifying delafossite silver ferrite with polyaniline: Visible-light-response Z-scheme heterojunction with charge transfer driven by internal electric field. *Chem. Eng. J.* **2019**, *370*, 1087–1100. [[CrossRef](#)]
41. Janczarek, M.; Kowalska, E. On the origin of enhanced photocatalytic activity of copper-modified titania in the oxidative reaction systems. *Catalysts* **2017**, *7*, 317. [[CrossRef](#)]
42. Bessekhouad, Y.; Robert, D.; Weber, J.V. Bi₂S₃/TiO₂ and CdS/TiO₂ heterojunctions as an available configuration for photocatalytic degradation of organic pollutant. *J. Photochem. Photobiol. A* **2004**, *163*, 569–580. [[CrossRef](#)]
43. Marschall, R. Semiconductor composites: Strategies for enhancing charge carrier separation to improve photocatalytic activity. *Adv. Funct. Mater.* **2014**, *24*, 2421–2440. [[CrossRef](#)]
44. Sharma, S.; Khare, N. Sensitization of narrow band gap Bi₂S₃ hierarchical nanostructures with polyaniline for its enhanced visible-light photocatalytic performance. *Colloid Polym. Sci.* **2018**, *296*, 1479–1489. [[CrossRef](#)]
45. Mou, J.; Xu, Y.; Zhong, D.; Chang, H.; Li, J.; Xu, C.; Wang, H.; Shen, H. A highly efficient visible-light-driven photocatalytic fuel cell with ZnIn₂S₄/PANI/TiO₂/Ti photoanode for simultaneous degradation of rhodamine B and electricity generation. *New J. Chem.* **2023**, *47*, 4277–4287. [[CrossRef](#)]
46. Feizpoor, S.; Habibi-Yangjeh, A.; Yubuta, K.; Vadivel, S. Fabrication of TiO₂/CoMoO₄/PANI nanocomposites with enhanced photocatalytic performances for removal of organic and inorganic pollutants under visible light. *Mater. Chem. Phys.* **2019**, *224*, 10–21. [[CrossRef](#)]
47. Li, W.; Tian, Y.; Zhao, C.; Zhang, Q.; Geng, W. Synthesis of magnetically separable Fe₃O₄ at PANI/TiO₂ photocatalyst with fast charge migration for photodegradation of EDTA under visible-light irradiation. *Chem. Eng. J.* **2016**, *303*, 282–291. [[CrossRef](#)]
48. Sharma, S.; Sharma, A.; Chauhan, N.; Tahir, M.; Kumari, K.; Mittal, A.; Kumar, N. TiO₂/Bi₂O₃/PANI nanocomposite materials for enhanced photocatalytic decontamination of organic pollutants. *Inorg. Chem. Commun.* **2022**, *146*, 110093.
49. Zeynali, S.; Taghizadeh, M.T. Highly efficient TiO₂/AgBr/PANI heterojunction with enhanced visible light photocatalytic activity towards degradation of organic dyes. *J. Mater. Sci. Mater. Electron.* **2019**, *30*, 17020–17031. [[CrossRef](#)]
50. Zhao, J.; Biswas, M.R.U.D.; Oh, W.-C. A novel BiVO₄-GO-TiO₂-PANI composite for upgraded photocatalytic performance under visible light and its non-toxicity. *Environ. Sci. Pollut. Res.* **2019**, *26*, 11888–11904. [[CrossRef](#)]
51. Zhou, Q.; Zhao, D.; Sun, Y.; Sheng, X.; Zhao, J.; Guo, J.; Zhou, B. g-C₃N₄-and polyaniline-co-modified TiO₂ nanotube arrays for significantly enhanced photocatalytic degradation of tetrabromobisphenol A under visible light. *Chemosphere* **2020**, *252*, 126468. [[CrossRef](#)]
52. Zarrin, S.; Heshmatpour, F. Photocatalytic activity of TiO₂/Nb₂O₅/PANI and TiO₂/Nb₂O₅/RGO as new nanocomposites for degradation of organic pollutants. *J. Hazard. Mater.* **2018**, *351*, 147–159. [[CrossRef](#)]
53. Wang, Y.; Zhang, P.; Zhang, T.C.; Xiang, G.; Wang, X.; Pehkonen, S.; Yuan, S. A magnetic γ-Fe₂O₃@PANI@TiO₂ core-shell nanocomposite for arsenic removal via a coupled visible-light-induced photocatalytic oxidation-adsorption process. *Nanoscale Adv.* **2020**, *2*, 2018–2024. [[CrossRef](#)]
54. Nekooie, R.; Shamspur, T.; Mostafavi, A. Novel CuO/TiO₂/PANI nanocomposite: Preparation and photocatalytic investigation for chlorpyrifos degradation in water under visible light irradiation. *J. Photochem. Photobiol. A* **2021**, *407*, 113038. [[CrossRef](#)]
55. Mousli, F.; Chaouchi, A.; Jouini, M.; Maurel, F.; Kadri, A.; Chehimi, M.M. Polyaniline-grafted RuO₂-TiO₂ heterostructure for the catalysed degradation of methyl orange in darkness. *Catalysts* **2019**, *9*, 578. [[CrossRef](#)]
56. Alenizi, M.A.; Rajeev, K.; Aslam, M.; Alseroury, F.A.; Barakat, M.A. Construction of a ternary g-C₃N₄/TiO₂@polyaniline nanocomposite for the enhanced photocatalytic activity under solar light. *Sci. Rep.* **2019**, *9*, 12091. [[CrossRef](#)] [[PubMed](#)]
57. Zhang, H.; Zong, R.; Zhao, J.; Zhu, Y. Dramatic visible photocatalytic degradation performances due to synergetic effect of TiO₂ with PANI. *Environ. Sci. Technol.* **2008**, *42*, 3803–3807. [[CrossRef](#)]
58. Zhang, H.; Tao, Z.; Tang, Y.; Yang, M.; Wang, G. One-step modified method for a highly efficient Au-PANI@TiO₂ visible-light photocatalyst. *New J. Chem.* **2016**, *40*, 8587–8592. [[CrossRef](#)]
59. Yu, Q.-Z.; Wang, M.; Chen, H.-Z.; Dai, Z.-W. Polyaniline nanowires on TiO₂ nano/microfiber hierarchical nano/microstructures: Preparation and their photocatalytic properties. *Mater. Chem. Phys.* **2011**, *129*, 666–672. [[CrossRef](#)]
60. Zhou, T.; Ma, L.; Gan, M.; Wang, H.; Hao, C. Sandwich-structured hybrids: A facile electrostatic self-assembly of exfoliated titania nanosheets and polyaniline nanoparticles and its high visible-light photocatalytic performance. *J. Phys. Chem. Solids* **2019**, *125*, 123–130. [[CrossRef](#)]

61. El-Bery, H.M.; Salah, M.R.; Ahmed, S.M.; Soliman, S.A. Efficient non-metal based conducting polymers for photocatalytic hydrogen production: Comparative study between polyaniline, polypyrrole and PEDOT. *RSC Adv.* **2021**, *11*, 13229. [[CrossRef](#)]
62. Cionti, C.; Pina, C.D.; Meroni, D.; Falletta, E.; Ardizzone, S. Triply green polyaniline: UV irradiation-induced synthesis of a highly porous PANI/TiO₂ composite and its application in dye removal. *Chem. Commun.* **2018**, *54*, 10702–10705. [[CrossRef](#)] [[PubMed](#)]
63. Li, J.; Zhu, L.; Wu, Y.; Harima, Y.; Zhang, A.; Tang, H. Hybrid composites of conductive polyaniline and nanocrystalline titanium oxide prepared via self-assembling and graft polymerization. *Polymer* **2006**, *47*, 7361–7367. [[CrossRef](#)]
64. Liao, G.; Chen, S.; Quan, X.; Zhang, Y.; Zhao, H. Remarkable improvement of visible light photocatalysis with PANI modified core-shell mesoporous TiO₂ microspheres. *Appl. Catal. B Environ.* **2011**, *102*, 126–131. [[CrossRef](#)]
65. Deng, Y.; Tang, L.; Zeng, G.; Dong, H.; Yan, M.; Wang, J.; Hu, W.; Wang, J.; Zhou, Y.; Tang, J. Enhanced visible light photocatalytic performance of polyaniline modified mesoporous single crystal TiO₂ microsphere. *Appl. Surf. Sci.* **2016**, *387*, 882–893. [[CrossRef](#)]
66. Deng, X.; Chen, Y.; Wen, J.; Xu, Y.; Zhu, J.; Bian, Z. Polyaniline-TiO₂ composite photocatalysts for light-driven hexavalent chromium ions reduction. *Sci. Bull.* **2020**, *65*, 105–112. [[CrossRef](#)]
67. Guo, N.; Liang, Y.; Lan, S.; Liu, L.; Zhang, J.; Ji, G.; Gan, S. Microscale hierarchical three-dimensional flowerlike TiO₂/PANI composite: Synthesis, characterization, and its remarkable photocatalytic activity on organic dyes under UV-light and sunlight irradiation. *J. Phys. Chem. C* **2014**, *118*, 18343–18355. [[CrossRef](#)]
68. Cheng, Y.; An, L.; Gao, F.; Wang, G.; Li, X.; Chen, X. Simplified synthesis of polyaniline-TiO₂ composite nanotubes for removal of azo dyes in aqueous solution. *Res. Chem. Intermed.* **2013**, *39*, 3969–3979. [[CrossRef](#)]
69. Subramanian, M.N.; Goh, P.S.; Lau, W.J.; Ismail, A.F.; Gursoy, M.; Karaman, M. Synthesis of titania nanotubes/polyaniline via rotating bed-plasma enhanced chemical vapor deposition for enhanced visible light photodegradation. *Appl. Surf. Sci.* **2019**, *484*, 740–750. [[CrossRef](#)]
70. Liu, Z.; Miao, Y.; Liu, M.; Ding, Q.; Tjiu, W.W.; Cui, X.; Liu, T. Flexible polyaniline-coated TiO₂/SiO₂ nanofiber membranes with enhanced visible-light photocatalytic degradation performance. *J. Colloid Interface Sci.* **2014**, *424*, 49–55. [[CrossRef](#)]
71. Sambaza, S.S.; Maity, A.; Pillay, K. Polyaniline-coated TiO₂ nanorods for photocatalytic degradation of bisphenol A in water. *ACS Omega* **2020**, *5*, 29642–29656. [[CrossRef](#)]
72. Xu, S.; Han, Y.; Meng, H.; Xu, J.; Wu, J.; Xu, Y.; Zhang, X. Fabrication of polyaniline sensitized grey-TiO₂ nanocomposites and enhanced photocatalytic activity. *Sep. Purif. Technol.* **2017**, *184*, 248–256. [[CrossRef](#)]
73. Kavil, J.; Ullattil, S.G.; Alshahrie, A.; Periyat, P. Polyaniline as photocatalytic promoter in black anatase TiO₂. *Solar Energy* **2017**, *158*, 792–796. [[CrossRef](#)]
74. Gadgil, D.J.; Kodialbail, V.S. Suspended and polycaprolactone immobilized Ag@TiO₂/polyaniline nanocomposites for water disinfection and endotoxin degradation by visible and solar light-mediated photocatalysis. *Environ. Sci. Pollut. Res.* **2021**, *28*, 12780–12791. [[CrossRef](#)] [[PubMed](#)]
75. Galvao, R.A.; Silva, G.M.M.; Coelho, N.C.F.; Santa-Cruz, L.A.; Machado, G. Hydrogen production by the layer-by-layer assembled films of PANi TiO₂-AuNP. *Mater. Today Chem.* **2022**, *26*, 101072. [[CrossRef](#)]
76. Liu, X.; Lai, H.; Li, J.; Peng, G.; Yi, Z.; Zeng, R.; Wang, M.; Liu, Z. Polyaniline sensitized Pt@TiO₂ for visible-light-driven H₂ generation. *Int. J. Hydrogen Energy* **2019**, *44*, 4698–4706. [[CrossRef](#)]
77. Acosta-Alejandro, J.A.; Lopez-Gonzalez, R.; Frias-Marquez, D.M.; De La Rosa-Vazquez, J.M.; Uribe-Lopez, M.C.; Gomez, R. Polyaniline-sensitized SiO₂/TiO₂ photocatalysts for the degradation of phenol using visible light. *J. Photochem. Photobiol. A* **2022**, *425*, 113696. [[CrossRef](#)]
78. Ma, J.; Dai, J.; Duan, Y.; Zhang, J.; Qiang, L.; Xue, J. Fabrication of PANI-TiO₂/rGO hybrid composites for enhanced photocatalysis of pollutant removal and hydrogen production. *Renew. Energ.* **2020**, *156*, 1008–1018. [[CrossRef](#)]
79. Sulowska, A.; Wysocka, I.; Pelczarski, D.; Karczewski, J.; Zielińska-Jurek, A. Hybrid TiO₂-polyaniline photocatalysts and their application in building gypsum plasters. *Materials* **2020**, *13*, 1516. [[CrossRef](#)]
80. Monafared, A.H.; Jamshidi, M. Synthesis of polyaniline/titanium dioxide nanocomposite (PANI/TiO₂) and its application as photocatalyst in acrylic pseudo paint for benzene removal under UV/VIS lights. *Prog. Org. Coat.* **2019**, *136*, 105257. [[CrossRef](#)]
81. Yu, J.; Pang, Z.; Zheng, C.; Zhou, T.; Zhang, J.; Zhou, H.; Wei, Q. Cotton fabric finished by PANI/TiO₂ with multifunctions of conductivity, anti-ultraviolet and photocatalysis activity. *Appl. Surf. Sci.* **2019**, *470*, 84–90. [[CrossRef](#)]
82. Falletta, E.; Bruni, A.; Sartirana, M.; Boffito, D.C.; Cerrato, G.; Giordana, A.; Djellabi, R.; Khatibi, E.S.; Bianchi, C.L. Solar light photoactive floating polyaniline/TiO₂ composites for water remediation. *Nanomaterials* **2021**, *11*, 3071. [[CrossRef](#)] [[PubMed](#)]
83. Gu, L.; Wang, J.; Qi, R.; Wang, X.; Xu, P.; Han, X. A novel incorporating style of polyaniline/TiO₂ composites as effective visible photocatalysts. *J. Mol. Catal. A* **2012**, *357*, 19–25. [[CrossRef](#)]
84. Yan, X.; Ohno, T.; Nishijima, K.; Abe, R.; Ohtani, B. Is methylene blue an appropriate substrate for a photocatalytic activity test? A study with visible-light responsive titania. *Chem. Phys. Lett.* **2006**, *429*, 606–610. [[CrossRef](#)]
85. Hidalgo, D.; Bocchini, S.; Fontana, M.; Saracco, G.; Hernandez, S. Green and low-cost synthesis of PANI-TiO₂ nanocomposite mesoporous films for photoelectrochemical water splitting. *RSC Adv.* **2015**, *5*, 49429–49438. [[CrossRef](#)]
86. Teja, K.P.; Kodialbail, V.S. Visible light mediated photocatalytic reduction of CO₂ to non-fossil fuel and valuable products by polyaniline-TiO₂ nanocomposites. *Arab. J. Sci. Eng.* **2022**, *47*, 6591–6603. [[CrossRef](#)]
87. Kalikeri, S.; Kamath, N.; Gadgil, D.J.; Kodialbail, V.S. Visible light-induced photocatalytic degradation of Reactive Blue-19 over highly efficient polyaniline-TiO₂ nanocomposite: A comparative study with solar and UV photocatalysis. *Environ. Sci. Pollut. Res.* **2018**, *25*, 3731. [[CrossRef](#)]

88. Radoicic, M.; Saponjic, Z.; Jankovic, I.A.; Ciric-Marjanovic, G.; Ahrenkiel, S.P.; Comor, M.I. Improvements to the photocatalytic efficiency of polyaniline modified TiO₂ nanoparticles. *Appl. Catal. B Environ.* **2013**, *136–137*, 133–139. [[CrossRef](#)]
89. Salem, M.A.; Al-Ghonemiy, A.F.; Zaki, A.B. Photocatalytic degradation of Allura red and Quinoline yellow with Polyaniline/TiO₂ nanocomposite. *Appl. Catal. B Environ.* **2009**, *91*, 59–66. [[CrossRef](#)]
90. Wang, F.; Min, S.; Han, Y.; Feng, L. Visible-light-induced photocatalytic degradation of methylene blue with polyaniline-sensitized TiO₂ composite photocatalysts. *Superlattices Microstruct.* **2010**, *48*, 170–180. [[CrossRef](#)]
91. Lin, Y.; Li, D.; Hu, J.; Xiao, G.; Wang, J.; Li, W.; Fu, X. Highly efficient photocatalytic degradation of organic pollutants by PANI-modified TiO₂ composite. *J. Phys. Chem. C* **2012**, *116*, 5764–5772. [[CrossRef](#)]
92. Li, Y.; Yu, Y.; Wu, L.; Zhi, J. Processable polyaniline/titania nanocomposites with good photocatalytic and conductivity properties prepared via peroxo-titanium complex catalyzed emulsion polymerization approach. *Appl. Surf. Sci.* **2013**, *273*, 135–143. [[CrossRef](#)]
93. Jeong, W.-H.; Amna, T.; Ha, Y.-M.; Shamshi Hassan, M.; Kim, H.-C.; Khil, M.-S. Novel PANI nanotube@TiO₂ composite as efficient chemical and biological disinfectant. *Chem. Eng. J.* **2014**, *246*, 204–210. [[CrossRef](#)]
94. Subramanian, E.; Subbulakshmi, S.; Murugan, C. Inter-relationship between nanostructures of conducting polyaniline and the photocatalytic methylene blue dye degradation efficiencies of its hybrid composites with anatase TiO₂. *Mater. Res. Bull.* **2014**, *51*, 128–135. [[CrossRef](#)]
95. Sandhya, K.P.; Sugunan, S. Heterogeneous photocatalytic degradation of 4-nitrophenol by visible light responsive TiO₂-polyaniline nanocomposites. *J. Water Supply Res. Technol. AQUA* **2015**, *64*, 74–84. [[CrossRef](#)]
96. Reddy, K.R.; Karthik, K.V.; Benaka Prasad, S.B.; Soni, S.K.; Jeong, H.M.; Raghu, A.V. Enhanced photocatalytic activity of nanostructured titanium dioxide/polyaniline hybrid photocatalysts. *Polyhedron* **2016**, *120*, 169–174. [[CrossRef](#)]
97. Gilja, V.; Novakovic, K.; Travas-Sejdic, J.; Hrnjak-Murgic, Z.; Rokovic, M.K.; Zic, M. Stability and synergistic effect of polyaniline/TiO₂ photocatalysts in degradation of azo dye in wastewater. *Nanomaterials* **2017**, *7*, 412. [[CrossRef](#)]
98. Jumat, N.A.; Wai, P.S.; Ching, J.J.; Basirun, W.J. Synthesis of polyaniline-TiO₂ nanocomposites and their application in photocatalytic degradation. *Polym. Polym. Compos.* **2017**, *25*, 507–514. [[CrossRef](#)]
99. Radoicic, M.; Ciric-Marjanovic, G.; Spasojevic, V.; Ahrenkiel, S.P.; Mitric, M.N.; Novakovic, K.; Saponjic, Z. Superior photocatalytic properties of carbonized PANI/TiO₂ nanocomposites. *Appl. Catal. B Environ.* **2017**, *213*, 155–166. [[CrossRef](#)]
100. Yang, C.; Dong, W.; Cui, G.; Zhao, Y.; Shi, X.; Xia, X.; Tang, B.; Wang, W. Enhanced photocatalytic activity of PANI/TiO₂ due to their photosensitization-synergetic effect. *Electrochim. Acta* **2017**, *247*, 486–495. [[CrossRef](#)]
101. Cui, W.; He, J.; Wang, H.; Hu, J.; Liu, L.; Liang, Y. Polyaniline hybridization promotes photo-electro-catalytic removal of organic contaminants over 3D network structure of rGH-PANI/TiO₂ hydrogel. *Appl. Catal. B Environ.* **2018**, *232*, 232–245. [[CrossRef](#)]
102. Sojic Merkulov, D.V.; Despotovic, V.N.; Banic, N.D.; Armakovic, S.J.; Fincur, N.L.; Lazarevic, M.J.; Cetojevic-Simin, D.D.; Orcic, D.Z.; Radoicic, M.; Saponjic, Z.; et al. Photocatalytic decomposition of selected biologically active compounds in environmental waters using TiO₂/polyaniline nanocomposites: Kinetics, toxicity and intermediates assessment. *Environ. Pollut.* **2018**, *239*, 457–465. [[CrossRef](#)] [[PubMed](#)]
103. Rahman, K.H.; Kar, A.K. Effect of band gap variation and sensitization process of polyaniline (PANI)-TiO₂ p-n heterojunction photocatalysts on the enhancement of photocatalytic degradation of toxic methylene blue with UV irradiation. *J. Environ. Chem. Eng.* **2020**, *8*, 104181. [[CrossRef](#)]
104. Lal, S.D.; Jose, T.S.; Rajesh, C.; Puthukkara, P.A.R.; Unnikrishnan, K.S.; Arun, K.J. Accelerated photodegradation of polystyrene by TiO₂-polyaniline photocatalyst under UV radiation. *Eur. Polym. J.* **2021**, *153*, 110493.
105. Kumar, A.; Raorane, C.J.; Syed, A.; Bahkali, A.H.; Elgorban, A.M.; Raj, V.; Kim, S.C. Synthesis of TiO₂, TiO₂/PANI, TiO₂/PANI/GO nanocomposites and photodegradation of anionic dyes Rose Bengal and thymol blue in visible light. *Environ. Res.* **2023**, *216*, 114741. [[CrossRef](#)] [[PubMed](#)]
106. Uyguner-Demirel, C.S.; Turkten, N.; Karatas, Y.; Bekbolet, M. Photocatalytic performance of PANI modified TiO₂: Degradation of refractory organic matter. *Environ. Sci. Pollut. Res.* **2023**, *30*, 85626–85638. [[CrossRef](#)]

Disclaimer/Publisher's Note: The statements, opinions and data contained in all publications are solely those of the individual author(s) and contributor(s) and not of MDPI and/or the editor(s). MDPI and/or the editor(s) disclaim responsibility for any injury to people or property resulting from any ideas, methods, instructions or products referred to in the content.